AIMP3 Haploinsufficiency Disrupts Oncogene-Induced p53 Activation and Genomic Stability

Bum-Joon Park,[1] Young Sun Oh,[1] Seung Yong Park,[1] So Jung Choi,[1] Cornelia Rudolph,[2] Brigitte Schlegelberger,[2] and Sunghoon Kim[1]

[1]National Creative Research Initiatives Center for ARS Network, College of Pharmacy, Seoul National University, Seoul, Korea and [2]Institute for Cell and Molecular Pathology, Hannover Medical School, Hannover, Germany

Abstract

AIMP3 (previously known as p18) was shown to up-regulate p53 in response to DNA damage. Here, we show that AIMP3 couples oncogenic stresses to p53 activation to prevent cell transformation. Growth factor– or Ras-dependent induction of p53 was blocked by single allelic loss of AIMP3 as well as by suppression of AIMP3. AIMP3 heterozygous cells became susceptible to cell transformation induced by oncogenes such as Ras or Myc alone. The transformed AIMP3$^{+/-}$ cells showed severe abnormality in cell division and chromosomal structure. Thus, AIMP3 plays crucial roles in p53-mediated tumor-suppressive response against oncogenic stresses via differential activation of ATM and ATR, and in the maintenance of genomic stability. (Cancer Res 2006; 66(14): 6913-8)

Introduction

Oncogenic signals do not necessarily result in cell transformation because they are tightly linked to various tumor suppressive mechanisms that lead to apoptosis and premature senescence (1). Because the tumor suppressor p53 is known to play a critical role in this coupling (2, 3), the inactivating mutations of p53 or the inability to activate p53 would increase susceptibility to oncogene-induced chromosomal aberrations and cell transformation. p14/ARF (alternative reading frame product of p16; p19/ARF in mouse) has been suggested to play a major role in the linkage between the oncogenic stresses and p53 response (4, 5). However, there are accumulating cases in which oncogenes can induce p53-mediated apoptosis and tumor-suppressive response even in the absence of p14/ARF (6–8), implicating the presence of other pathways connecting oncogenic stresses and p53 activation. We recently showed that the aminoacyl-tRNA synthetase–interacting multifunctional protein, AIMP3 (previously known as p18), up-regulates p53 by directly activating ATM/ATR in response to DNA damage (9). Because ATM and ATR are the kinases responsible not only for DNA repair, but also for the regulation of the cell cycle (10), they are expected to respond to growth factors and oncogenes for the regulation of p53. Here, we tested whether AIMP3 can mediate the growth factor– or oncogene-induced signal pathway leading to p53 activation via ATM/ATR, and dissected how different types of oncogenic Ras are wired to p53. We also tested whether the cells devoid of one *AIMP3* allele would become more susceptible to oncogene-induced cell transformation and chromosomal destruction.

Materials and Methods

Materials and transfection. Mammalian expression vectors of Ras family and dominant-negative mutant, Ras17N, were kindly provided by S.G. Chi (Korea University). For transfection, we used Geneporter system, following the manufacturer's protocol. Other vectors used in this work were previously described (9). Cells were transfected with different types of oncogenic Ras, incubated for 20 hours, and harvested with radioimmunoprecipitation assay (RIPA) buffer. Proteins extracted from the cells were separated by SDS-PAGE and subjected to Western blot analysis with the indicated antibodies. The antibodies for p-Erk, p-p53 at S15, S20, and p-Chk2 were purchased from Cell Signaling, whereas p-Chk1 was from Santa Cruz Biotechnology (Santa Cruz, CA). To address the role of p19/ARF (kindly provided by H.W. Lee, Sungkyunkwan University), we transfected p19 into U2OS and incubated it for 24 hours. After washing the cells, we introduced Ras or Ras plus antisense AIMP3 into the cells and incubated it for an additional 8 hours.

Growth factor treatment. To test the effect of growth factors on the expression of AIMP3 and p53, we treated the indicated cells with 10 μg/mL of insulin-like growth factor-I (IGF-I; R&D Systems) or 2 μg/mL of vesicular endothelial cell growth factor-I (VEGF-I; R&D Systems) for 1 hour under serum-free conditions. After harvesting the cells with RIPA, proteins were separated by SDS-PAGE and subjected to Western blot analysis with anti-p53 (DO-1), -AIMP3, and -tubulin antibodies.

Western blot and immunoprecipitation. These procedures have been done as previously described (9). In brief, cells treated with IGF-I or VEGF-I for 2 hours were incubated with RIPA. After centrifugation, the proteins in the supernatants were separated by SDS-PAGE and subjected to Western blot analysis or incubated with anti-ATM (Santa Cruz Biotechnology) or anti-ATR (Serotec) antibody for 2 hours for immunoprecipitation. After an additional incubation for 1 hour with agarose-conjugated protein A or G, the precipitated proteins were subjected to Western blot with the specific antibodies.

Cell cycle analysis. Murine embryofibroblasts (MEF) were treated with IGF-I (20 μg/mL) for the indicated times and harvested with trypsin. After washing with PBS, the cells were fixed with 70% ethanol for 1 hour and stained with 50 μg/mL of propidium iodide solution in PBS. Twenty thousand cells per sample were used for fluorescence-activated cell sorting (FACS) analysis under the FL-2H detector using FACS scan. To determine the cell cycle distribution of the stable cell lines, we treated the cells with 10 μmol/L of nocodazole, or nocodazole and aphidicoline (4 μmol/L) for 6 hours. After harvesting the cells with trypsin, we stained the cells with propidium iodide and subjected it to FACS analysis.

Chemical inhibitors. U0126 (50 μmol/L), PD98059 (20 μmol/L), JNK inhibitor (20 μmol/L, Calbiochem, San Diego, CA), and SB203580 (10 μmol/L) were purchased from Calbiochem. Cells transfected with Ras for 18 hours were incubated with inhibitor-containing medium for 2 hours and harvested for Western blot analysis.

***In vitro* kinase assay.** We transfected H-Ras into 293 cells and Erk was immunoprecipitated with its specific antibody. GST-AIMP3 was purified and

Note: Supplementary data for this article are available at Cancer Research Online (http://cancerres.aacrjournals.org/).

B-J. Park and Y.S. Oh contributed equally to this work.

Requests for reprints: Sunghoon Kim, National Creative Research Initiatives Center for ARS Network, College of Pharmacy, Seoul National University, Seoul 151-742, Korea. Phone: 822-880-8180; Fax: 822-875-2620; E-mail: sungkim@snu.ac.kr.

doi:10.1158/0008-5472.CAN-05-3740

incubated with the immunoprecipitated Erk in the kinase buffer containing 20 mmol/L of Tris-HCl (pH 7.5), 0.1 mmol/L of EGTA, 3 mmol/L of DTT, 2.5 mmol/L of $MgCl_2$, and 10 μmol/L of ATP at room temperature for 10 minutes. The reaction mixtures were subjected to Western blot analysis with phosphothreonine, phosphoserine, and phosphotyrosine antibodies.

Immunostaining. Cells were seeded on a cover glass and transfected with Ras. After fixation with ice-cold 100% methanol, the glass was incubated with blocking buffer (PBS, 0.01% bovine serum albumin, and 0.05% Triton X-100) for 1 hour. After washing with PBST, the cells were reacted with the primary antibody (1:200), and subsequently with the FITC-conjugated secondary antibody (1:1,000). The cells were then stained with propidium iodide, and observed using confocal microscopy (μ-Radiance; Bio-Rad, Hercules, CA).

Cell immortalization. 13.5d $AIMP3^{+/+}$ and $AIMP3^{+/-}$ MEFs were transfected with EV, H-Ras12V, c-Myc, and Ras12V/c-Myc for 48 hours, and selected against G418 (400 μg/mL) for 1 week. After removing untransfected cells, the transfected cells were divided into two dishes. Then the cells in one dish were Giemsa-stained and those in the other dish were cultured for an additional 2 weeks in the G418-containing medium.

Cell proliferation and anchorage-independent growth. To determine the significance of AIMP3 for cell proliferation, $AIMP3^{+/+}$ and $AIMP3^{+/-}$ cells were seeded at 1.8×10^4 cells/well in serum-free medium containing IGF-I (10 μg/mL) or VEGF-I (2 μg/mL) for 3 days. The cells were counted at 24-hour intervals for a period of 72 hours. Cell viability was determined by trypan blue exclusion assay. For the measurement of anchorage-independent cell growth, cells were mixed with 0.8% low-melting agarose containing DMEM and plated into uncoated culture dishes. After 5 days of incubation, we fixed the cells using 1% PFA and counted the colonies on the plates.

Chromosome preparation. For the preparation of metaphase chromosomes, cells were treated with colcemid at a concentration of 0.035 μg/mL, incubated in 0.075 mol/L KCl for 30 minutes at 37°C, and fixed in a freshly prepared solution of methanol/acetic acid (3:1) at room temperature. The cell suspension was dropped onto glass slides in a climate chamber (Polymer, Kassel, Germany) at 22°C and 48% humidity.

Spectral karyotyping. Cytogenetic characterization using spectral karyotyping (SKY) was carried out as previously described (11). In brief, metaphase spreads were hybridized with the SKY probe mixture for mouse chromosomes and signal detection was done according to the manufacturer's instructions (Applied Spectral Imaging, Migdal HaEmek, Israel). Chromosomes were counterstained with 4,6-diamidino-2-phenylindole and mounted with Vectashield (Vector Laboratories, Burlingame, CA). For image acquisition and karyotyping, the SpectraCube system (Applied Spectral Imaging) coupled to an epifluorescence microscope with CCD camera and SkyView software (Applied Spectral Imaging) were used. A total of 14 or 15 metaphases per case were analyzed.

Results and Discussion

To understand the regulation of AIMP3 in response to growth signals, we first checked whether AIMP3 levels are changed by growth factors such as IGF-I and VEGF-I (12, 13). Both of these growth factors induced AIMP3 as well as p53 in HCT116 cells as determined by Western blotting (Fig. 1*A*), and immunofluorescence staining (Supplementary Fig. S1*A*). The growth factor–dependent induction of AIMP3 was also observed in $AIMP3^{+/+}$, but not in $AIMP3^{+/-}$ MEFs in which AIMP3 levels were reduced (Fig. 1*B*; Supplementary Fig. S1*B*), demonstrating the importance of AIMP3 for the up-regulation of p53. We then suppressed AIMP3 with its antisense RNA, and checked the induction of p53 in response to IGF-I and VEGF-I. The growth factor–dependent induction of AIMP3 and p53 was both suppressed with AIMP3 antisense RNA (Fig. 1*C*). We previously reported the stimulatory interaction of AIMP3 with ATM that is the activating kinase of p53 (9). Here, we checked the growth factor–dependent binding of AIMP3 to ATM. As expected, the treatment of IGF-I and VEGF-I increased the interaction of AIMP3 with ATM, which was blocked with AS-AIMP3 (Fig. 1*D*). To further confirm whether the precipitation of AIMP3 is dependent on ATM, we used the ATM-deficient cell line, AT22IJE-T, transfected with empty vector or ATM and did the same coimmunoprecipitation experiment. AIMP3 was coimmunoprecipitated with ATM in the ATM-transfected cells, but not in ATM-negative cells (Supplementary Fig. S1*C*). We then compared the cell cycle progression between $AIMP3^{+/+}$ and $AIMP3^{+/-}$ MEFs after IGF-I treatment in the starving condition. In the wild-type MEFs, IGF-I transiently promoted the cell cycle, but the portion of the G_1 phase cells was increased in later stage, whereas $AIMP3^{+/-}$ MEFs were less sensitive to the IGF-I treatment (Fig. 1*E*). We also compared the response of the two cells to the proliferation signals by cell counting. Although the number of viable $AIMP3^{+/+}$ MEFs were rapidly decreased after the growth factor treatment, $AIMP3^{+/-}$ cells were kept alive (Fig. 1*F*), further supporting the importance of AIMP3 in cell cycle control.

Because IGF-I and VEGF-I induce the Ras-MAPK pathway (12, 13), we checked whether AIMP3 is also induced by oncogenic mutant H-Ras (H-Ras12V). Transfection of H-Ras12V induced AIMP3 as well as p53 in MCF-7, and the suppression of AIMP3 with AS-AIMP3 inhibited the induction of p53 (Fig. 2*A*). Because Ras could activate MAPKs (14), we determined the specific MAPK that is responsible for the induction of AIMP3 and p53 using chemical inhibitors. When the cells were pretreated with chemical inhibitors, U0126 and SB203580 for Erk and p38 MAPK, respectively, and I-JNK for JNK, the induction of AIMP3 and p53 was blocked by the treatment of U0126, but not with the two other MAPK inhibitors, suggesting that Erk is responsible for the Ras-dependent enhancement of AIMP3 and p53 (Supplementary Fig. S2). The induction of p53 was also blocked with another known inhibitor of Erk, PD98059 (Fig. 2*B*), further confirming the involvement of Erk. To see whether AIMP3 would be a direct substrate of Erk, we did an *in vitro* kinase assay. Erk was immunoprecipitated with its antibody from 293 cells transfected with H-Ras, and incubated with GST-AIMP3 for the kinase reaction. The phosphorylation of AIMP3 was then determined by Western blotting with the antibodies against phosphoserine, phosphothreonine, and phosphotyrosine. H-Ras increased the phosphorylation of AIMP3 at all of these residues, which were suppressed by the treatment of PD98059 (Fig. 2*C*), suggesting AIMP3 as a direct substrate of Erk. To address the engagement of ATM in this signal pathway, we checked the p53 response against H-Ras in an ATM-deficient cell line (15). The Ras-dependent induction of p53 was not observed in the ATM-negative cells (Fig. 2*D*). However, in both cell lines, AIMP3 was induced by Ras, suggesting that the induction of AIMP3 does not require ATM.

Because p14/ARF has been suggested as the mediator in the oncogene-mediated p53 activation through the suppression of MDM2 (16), we determined the engagement of p14/ARF in the Ras-dependent induction of p53 by testing whether Ras as well as growth factors could still activate p53 in a p14-deficient human osteosarcoma cell line, U2OS (17). Both AIMP3 and p53 were induced by growth factors and H-Ras in this cell line (Fig. 2*E*), implying that p14/ARF is not the sole conduit linking Ras to p53 at least in human case. We then introduced p19/ARF into U2OS cells to reestablish this pathway but suppressed AIMP3 with AS-AIMP3, and checked whether Ras-induced activation of p53 would occur by the restoration of the ARF pathway independently of AIMP3. The induction of p53 by Ras was not observed in U2OS cells when AIMP3 was suppressed with its antisense RNA, even if ARF was restored by transfection (Fig. 2*F*). This indicates that ARF is not

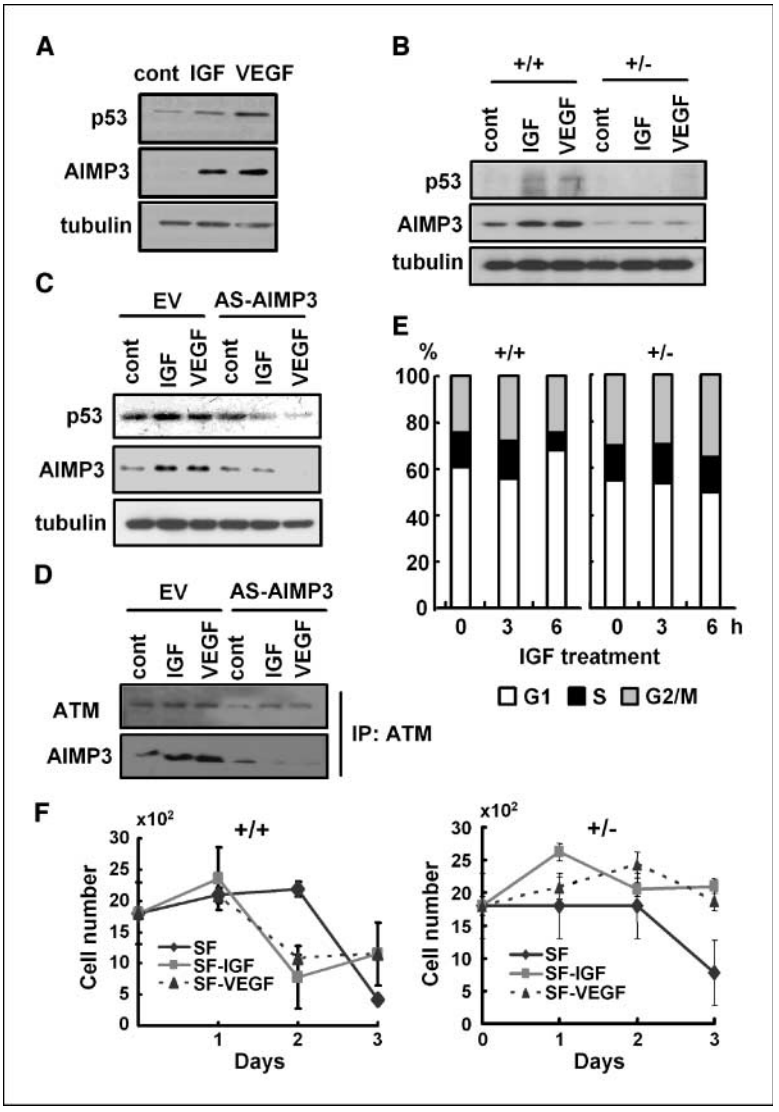

Figure 1. AIMP3 is critical for growth factor–dependent p53 induction and growth arrest under starving conditions. *A,* HCT116 cells were incubated with IGF-I or VEGF-I, and the induction of AIMP3 and p53 was checked by Western blotting with their specific antibodies as described in Materials and Methods. *B,* AIMP3$^{+/+}$ and AIMP3$^{+/-}$ MEFs were treated with growth factors, and the AIMP3 and p53 levels were determined by Western blotting. *C,* 293 cells were transfected with empty vector (*EV*) or antisense AIMP3 (*AS-AIMP3*) for 24 hours, treated with IGF and VEGF, and subjected to Western blot analysis as above. *D,* the interaction of AIMP3 with ATM was determined by coimmunoprecipitation of AIMP3 with ATM at the same condition as above. *E,* MEFs were treated with IGF-I for 3 and 6 hours under the serum-free condition, and cell cycle progression was analyzed by flow cytometry. *F,* AIMP3$^{+/+}$ and AIMP3$^{+/-}$ MEFs were treated with IGF-I or VEGF-I under the serum-free condition, collected at 1-day intervals for 3 days, and the viable cells were measured by trypan blue counting.

sufficient for the restoration of p53 response to Ras without AIMP3, further supporting the importance of AIMP3 in the mediation of Ras signal to p53.

We next checked the effect of three different Ras subfamilies (18) on the induction of AIMP3 and p53. All three different types of Ras increased the level of AIMP3 and p53, as well as the phosphorylation of Erk, as determined by Western blotting (Fig. 3*A*) and immunofluorescence staining (Fig. 3*B*). Although different oncogenic types of Ras give similar effects on cell cycle, each Ras seems to have different mutation frequencies depending on the cancer type (18). We thus investigated whether the three different Ras subfamilies were distinguished in the AIMP3-dependent activation of p53. To address this possibility, we transfected each Ras and checked the phosphorylation of p53. H-Ras augmented the phosphorylation of p53 at serine 15, whereas N- and K-Ras enhanced the phosphorylation of p53 at serine 20 and serine 15 (Fig. 3*C*). Next, we checked the Ras-dependent interaction of AIMP3 with ATM and ATR. H-Ras and K-/N-Ras increased the interaction of AIMP3 with ATM and ATR, respectively (Fig. 3*D*). Then, ATM and ATR were inhibited by the introduction of their kinase-dead (KD) mutants, and a Ras-dependent p53 induction was observed. ATM-KD and ATR-KD blocked the p53 induction by H- and N-/K-Ras, respectively (Fig. 3*E*). To further confirm this specificity, we checked the Ras-dependent phosphorylation of Chk1 and Chk2 that are the downstream substrates of ATR and ATM, respectively (10). As expected, H- and K-/N-Ras enhanced the phosphorylation of Chk2 and Chk1, respectively (Fig. 3*F*). All of these results suggest that the target specificity of AIMP3 between ATM and ATR would be determined by the types of Ras.

AIMP3 is expected to play a pivotal role in the suppression of oncogenic cell transformation because it links the oncogenic signal to tumor suppressive response mediated by p53. This possibility was tested by comparing the susceptibility of AIMP3$^{+/+}$ and AIMP3$^{+/-}$ MEFs to oncogene-induced transformation using H-Ras or c-Myc. In the AIMP3$^{+/+}$ MEFs, the stable cells were generated only by the introduction of Ras and Myc, but not by each alone (Fig. 4*A, top row*). In contrast, AIMP3$^{+/-}$ MEFs were transformed by the transfection of Ras or Myc alone. Transfection of both Ras and Myc into AIMP3$^{+/-}$ MEFs induced severe cell death, perhaps due to the reduced tolerance against oncogenic stresses (Fig. 4*A, bottom row*). We further confirmed the single oncogene-induced transformation of AIMP3$^{+/-}$ cells by colony-forming assay (Supplementary Fig. S3*A*), anchorage-independent growth (Fig. 4*B*), and cell growth rate assays (Supplementary Fig. S3*B*).

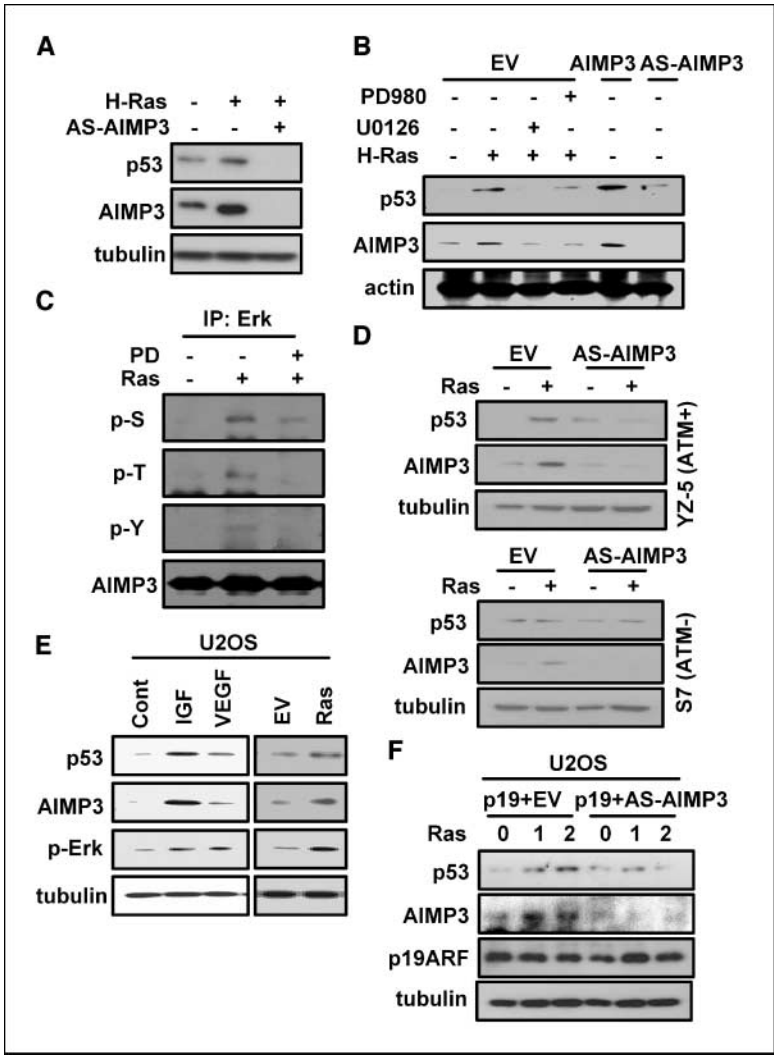

Figure 2. Functional importance of AIMP3 in Ras-dependent induction of p53. *A,* MCF-7 cells were transfected with oncogenic mutant, H-Ras12V, or AS-AIMP3, and the AIMP3 and p53 levels were compared by Western blotting. *B,* HCT116 cells were transfected with the indicated vectors and treated with the Erk inhibitors (50 μmol/L U0126 or 10 μmol/L PD98059) for 2 hours before harvest. AIMP3 and AS-AIMP3 were transfected as the positive and negative controls, respectively. *C,* 293 cells were transfected with H-Ras with or without treatment of PD98059 for 2 hours. Erk was immunoprecipitated with its specific antibody and incubated with the purified GST-AIMP3. The phosphorylation of GST-AIMP3 was determined by Western blotting with anti-phosphoserine, phosphothreonine, and phosphotyrosine antibodies. *D,* to determine the involvement of ATM in the AIMP3-dependent induction of p53, H-Ras, or EV was transfected to the isogenic ATM-negative AT22JE-T S7 and ATM-positive YZ-5 cell lines (15). AS-AIMP3 was introduced to see the requirement of AIMP3 for the induction of p53. *E,* the effect of growth factors and H-Ras on the induction of p53, AIMP3, and the activation of Erk was determined by Western blotting in p14/ARF-deficient U2OS cells. *F,* to determine the significance of AIMP3 and p19/ARF in the Ras-dependent induction of p53, U2OS cells were transfected with p19/ARF together with EV or AS-AIMP3, and the p53 and AIMP3 levels were determined by Western blotting.

We checked an abnormality in cell division of AIMP3$^{+/-}$ stable cell lines resulting from the disrupted cell cycle control. The AIMP3$^{+/-}$ stable cells showed uneven cell division at high frequency (Fig. 4*C, arrows*). These cells also contained enlarged or fragmented nuclei, whereas the AIMP3$^{+/+}$ stable cells transformed with Ras and Myc showed normal nuclear morphology (Supplementary Fig. S3*C* and *D*). Moreover, Ras- or Myc-transformed AIMP3$^{+/-}$ cells often showed an impairment in mitotic chromosomal alignment and segregation (Supplementary Fig. S3*E*). We further investigated chromosomal aberration in the AIMP3$^{+/-}$ stable cell lines using SKY analysis as previously described (11). Chromosome deletion, duplication, and unbalanced translocations were found in various chromosomes in Ras- or Myc-transformed AIMP3$^{+/-}$ cells (see Supplementary Table S1 and Fig. S4*D* for details). All of these results suggest that AIMP3 is required for chromosomal stability.

Next, we checked the possible abnormality in cell cycle control using chemical inhibitors of cell cycle progression. Although the Ras + Myc–transformed AIMP3$^{+/+}$ stable cells responded to the G_2-M arrest by nocodazole and S phase arrest by aphidicolin, the Ras- or Myc-transformed AIMP3$^{+/-}$ stable cells were insensitive to these chemicals (Fig. 4*E*). Moreover, the G_1 peaks of the AIMP3$^{+/-}$-stable cells were shifted rightward compared with that of the AIMP3$^{+/+}$ cells, further supporting the enlarged nuclear structures (Supplementary Fig. S3*C*). The two kinases, Chk1 or Chk2, responsible for the chemically induced cell cycle arrest, were not activated in the Ras- or Myc-transformed AIMP3$^{+/-}$ cells (Supplementary Fig. S4), consistent with the results of FACS analysis (Fig. 4*E*). All of these results show that AIMP3 is a critical cell cycle regulator and safeguard against oncogene-induced cell transformation.

The chromosome instability and uncontrolled cell cycle shown in the Ras- or Myc-transfected AIMP3$^{+/-}$ cells gives some insight into the reduced transformation efficiency shown in the Ras + Myc double-transfected AIMP3$^{+/-}$ cells (Fig. 4*A*). The strong growth promotion spurred by double oncogenic signals with reduced DNA repairing capability could accumulate many critical mutations that would lead to the death of AIMP3$^{+/-}$ cells.

It is well known that oncogenic stresses are normally counteracted by the accompanying induction of tumor suppressors such as Rb and p53 (19). Here, we elucidated that AIMP3 is critical for the response of p53 to Ras via its activation of ATM/ATR (Fig. 2). We previously showed the specific interaction of AIMP3 with the FAT domain of ATM and ATR (9). Interestingly, whereas our previous work showed that the suppression of AIMP3 accompanies the down-regulation of ATM, here, the reverse seems to be the case

(Fig. 1*C*). Thus, the expression levels of ATM and AIMP3 seem to be linked together through an unknown feedback mechanism. In this regard, it is noteworthy that the AIMP3 promoter contains a potential binding site for E2F-1 that is induced by ATM upon DNA damage, and ATM itself is also regulated by E2F-1 (20). The possible involvement of E2F-1 in the regulation of ATM and AIMP3 needs further investigation.

Moreover, we showed that AIMP3 differentially regulates ATM and ATR depending on the type of Ras (Fig. 3*C-F*). It is not clear at this moment whether AIMP3 itself can discern between the two target kinases or is differentially guided by Ras signal. H-Ras promotes the G_1-S transition in which ATM serves as a critical checkpoint, whereas N- and K-Ras are involved in the S-G_2-M phase in which ATR predominantly works for the activation of checkpoint signaling (21, 22). Thus, AIMP3 may be differently guided between ATM and ATR depending on the Ras signal. This work also elucidated that the reduction of AIMP3 renders the cells susceptible to transformation by single oncogenes and induces genomic instability (Fig. 4; Supplementary Fig. S3; Table S1). The cellular and genomic characteristics shown in the AIMP3$^{+/-}$ stable cells would provide important information on the tumorigenic process resulting from the disruption of AIMP3 expression or activity.

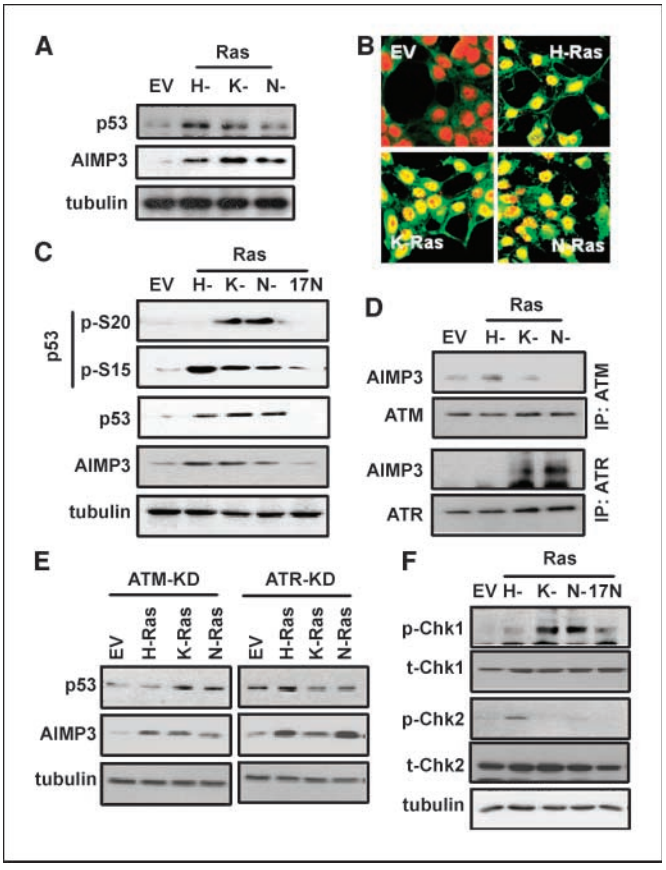

Figure 3. Ras-induced differential activation of ATM and ATR via AIMP3. *A,* three different oncogenic forms of Ras (H-, K-, and N-) were transfected into 293 cells for 24 hours and their effect on the levels of p53 and AIMP3 was determined by Western blotting. Tubulin was used as a loading control. *B,* the effect of Ras on the induction and cellular localization of AIMP3 was monitored by immunofluorescence staining of 293 cells. *C,* the effect of each Ras was checked in 293 cells on the phosphorylation of p53 at Ser15 and 20 by Western blotting with their specific antibodies. The dominant-negative mutant Ras17N (23) was used as a negative control. *D,* each Ras was introduced into 293 cells with Flag-ATM or -ATR, and the interaction of AIMP3 with ATM and ATR was monitored by coimmunoprecipitation with anti-Flag antibody. *E,* the effect of kinase-dead (KD) mutants of ATM or ATR were determined on the induction of p53 and AIMP3 in 293 cells. *F,* the effect of each Ras was determined in 293 cells on the phosphorylation of Chk1 and Chk2 that are the target substrates of ATR and ATM, respectively, by Western blotting with their specific antibodies. The total Chk1 and 2 were also determined with their specific antibodies.

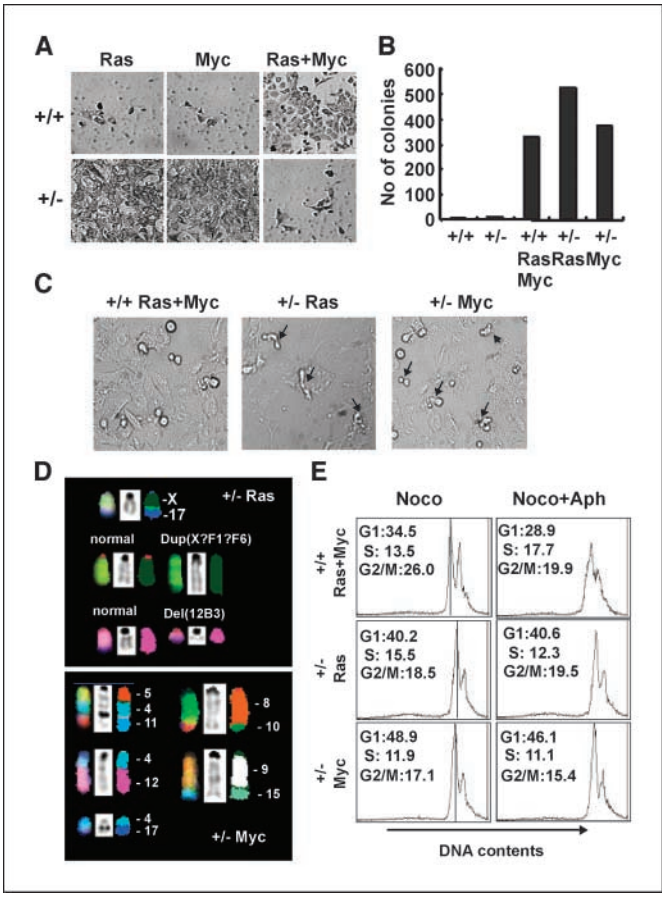

Figure 4. Immortalization and chromosomal aberration of AIMP3$^{+/-}$ cells induced by single oncogene. *A,* MEF cells were transfected with H-Ras and c-Myc, and the surviving cells were selected with G418 (400 μg/mL) for 1 month. The selected stable cells were photographed under light microscopy (×100). *B,* the stable cells were seeded on soft agar and the colonies were counted as described in Materials and Methods. *C,* morphology of dividing cells observed by light microscopy (×200). *Arrows,* unevenly dividing cells. *D,* clonal alterations in chromosome structure of Ras- or Myc-transformed AIMP3$^{+/-}$ cells are shown by SKY analysis. Ras-transformed AIMP3$^{+/-}$ cells show chromosome aberrations such as unbalanced translocation between chromosomes X and 17, duplication in chromosome X, and deletion in chromosome 12. Myc-transformed cells contained dicentric chromosome Dic(4;11) with the breakpoint at 4C4, and additional translocation with chromosome 5, unbalanced translocations between chromosomes 8/10 and 4/12 with the breakpoint at 4A5, 9/15, and 4/17. Further description in chromosomal aberrations was summarized in Supplementary Table S1. *E,* MEFs were treated with nocodazole for 6 hours (to activate Chk1 for G_2-M phase arrest) or aphidicolin (to activate Chk2 for G_1-S arrest) in addition to nocodazole for 6 hours to see how the AIMP3$^{+/+}$ and AIMP3$^{+/-}$ stable cells would respond to G_2-M and S phase arrest. Although Ras + Myc-transformed AIMP3$^{+/+}$ stable cells responded to G_1-S and G_2-M arrest, Ras- or Myc-transformed AIMP3$^{+/-}$ cells were not arrested by the chemical treatment. Notice that the enlargement of nuclei in the heterozygous cell lines is shown by the rightward shift of the G_1 peaks compared with that of the wild-type cell line (*vertical lines*).

Acknowledgments

Received 10/17/2005; revised 4/17/2006; accepted 5/31/2006.

The costs of publication of this article were defrayed in part by the payment of page charges. This article must therefore be hereby marked *advertisement* in accordance with 18 U.S.C. Section 1734 solely to indicate this fact.

References

1. Lowe SW, Cepero E, Evan G. Intrinsic tumour suppression. Nature 2004;432:307–15.
2. Serrano M, Lin AW, McCurrach ME, Beach D, Lowe SW. Oncogenic ras provokes premature cell senescence associated with accumulation of p53 and p16INK4a. Cell 1997;88:593–602.
3. Selivanova G. p53: fighting cancer. Curr Cancer Drug Targets 2004;4:385–402.
4. Lowe SW, Sherr CJ. Tumor suppression by Ink4a-Arf: progress and puzzles. Curr Opin Genet Dev 2003;13:77–83.
5. Sherr CJ. The INK4a/ARF network in tumour suppression. Nat Rev Mol Cell Biol 2001;2:731–7.
6. Verschuren EW, Klefstrom J, Evan GI, Jones N. The oncogenic potential of Kaposi's sarcoma-associated herpesvirus cyclin is exposed by p53 loss *in vitro* and *in vivo*. Cancer Cell 2002;2:229–41.
7. Tolbert D, Lu X, Yin C, Tantama M, Van Dyke T. p19(ARF) is dispensable for oncogenic stress-induced p53-mediated apoptosis and tumor suppression *in vivo*. Mol Cell Biol 2002;22:370–7.
8. Li Y, Wu D, Chen B, et al. ATM activity contributes to the tumor-suppressing functions of p14ARF. Oncogene 2004;23:7355–65.
9. Park BJ, Kang JW, Lee SW, et al. The haploinsufficient tumor suppressor AIMP3 upregulates p53 via interactions with ATM/ATR. Cell 2005;120:209–21.
10. Abraham RT. Cell cycle checkpoint signaling through the ATM and ATR kinases. Genes Dev 2001;15:2177–96.
11. Frank O, Rudolph C, Heberlein C, et al. Tumor cells escape suicide gene therapy by genetic and epigenetic instability. Blood 2004;104:3543–9.
12. Lu KH, Levine RA, Campisi J. c-ras-Ha gene expression is regulated by insulin or insulin-like growth factor and by epidermal growth factor in murine fibroblasts. Mol Cell Biol 1989;9:3411–7.
13. Yashima R, Abe M, Tanaka K, et al. Heterogeneity of the signal transduction pathways for VEGF-induced MAPKs activation in human vascular endothelial cells. J Cell Physiol 2001;188:201–10.
14. Pruitt K, Pruitt WM, Bilter GK, Westwick JK, Der CJ. Raf-independent deregulation of p38 and JNK mitogen-activated protein kinases are critical for Ras transformation. J Biol Chem 2002;277:31808–17.
15. Ziv Y, Jaspers NG, Etkin S, et al. Cellular and molecular characteristics of an immortalized ataxia-telangiectasia (group AB) cell line. Cancer Res 1989;49:2495–501.
16. Sharpless NE, DePinho RA. The INK4A/ARF locus and its two gene products. Curr Opin Genet Dev 1999;9:22–30.
17. Sandoval R, Xue J, Pilkinton M, Salvi D, Kiyokawa H, Colamonici OR. Different requirements for the cytostatic and apoptotic effects of type I interferons. Induction of apoptosis requires ARF but not p53 in osteosarcoma cell lines. J Biol Chem 2004;279:32275–80.
18. Adjei AA. Blocking oncogenic Ras signaling for cancer therapy. J Natl Cancer Inst 2001;93:1062–74.
19. Massague J. G1 cell-cycle control and cancer. Nature 2004;432:298–306.
20. Berkovich E, Ginsberg D. ATM is a target for positive regulation by E2F-1. Oncogene 2003;22:161–7.
21. Yang J, Yu Y, Hamrick HE, Duerksen-Hughes PJ. ATM, ATR and DNA-PK: initiators of the cellular genotoxic stress responses. Carcinogenesis 2003;24:1571–80.
22. Kastan MB, Bartek J. Cell-cycle checkpoints and cancer. Nature 2004;432:316–23.
23. Yamamoto-Honda R, Tobe K, Kaburagi Y, et al. Upstream mechanisms of glycogen synthase activation by insulin and insulin-like growth factor-I. Glycogen synthase activation is antagonized by wortmannin or LY294002 but not by rapamycin or by inhibiting p21ras. J Biol Chem 1995;270:2729–34.